CHAPTER 2

Experimental Apparatus

2.1 Introduction

All of the experiments presented in following chapters use the direct absorption of tunable single mode infrared laser radiation to probe molecular concentrations, quantum state distributions, and velocities. The infrared source is a modified Burliegh F-center laser (FCL) which is optically pumped at 647.1 nm with a Coherent Innova K3000 krypton ion laser. This section describes the experimental apparatus, particularly the IR spectrometer, starting with the Kr ion and F-center lasers. Manuals documenting typical operation are available for both lasers; the section below describes our modifications to these systems and a few practical hints to facilitate operation, alignment and maintenance. Later subsections describe ancillary equipment, diagnostics, signal detection, data acquisition, which comprise the spectrometer. The excimer laser based flash kinetic spectrometer and flow cell used in the Cl + HCl experiments are described in Chapter 3. A schematic overview of the IR spectrometer and crossed jet arrangement is shown in Fig. 2.1.

2.2 Kr ion laser

The Kr ion laser is the pump source for the FCL and, consequently, is the first source of noise as well. Amplitude noise on the red laser light can be particularly egregious as a result of poor optical alignment or incorrect tube pressure. Maximum power to noise ratio generally (and conveniently) coincides with maximum power

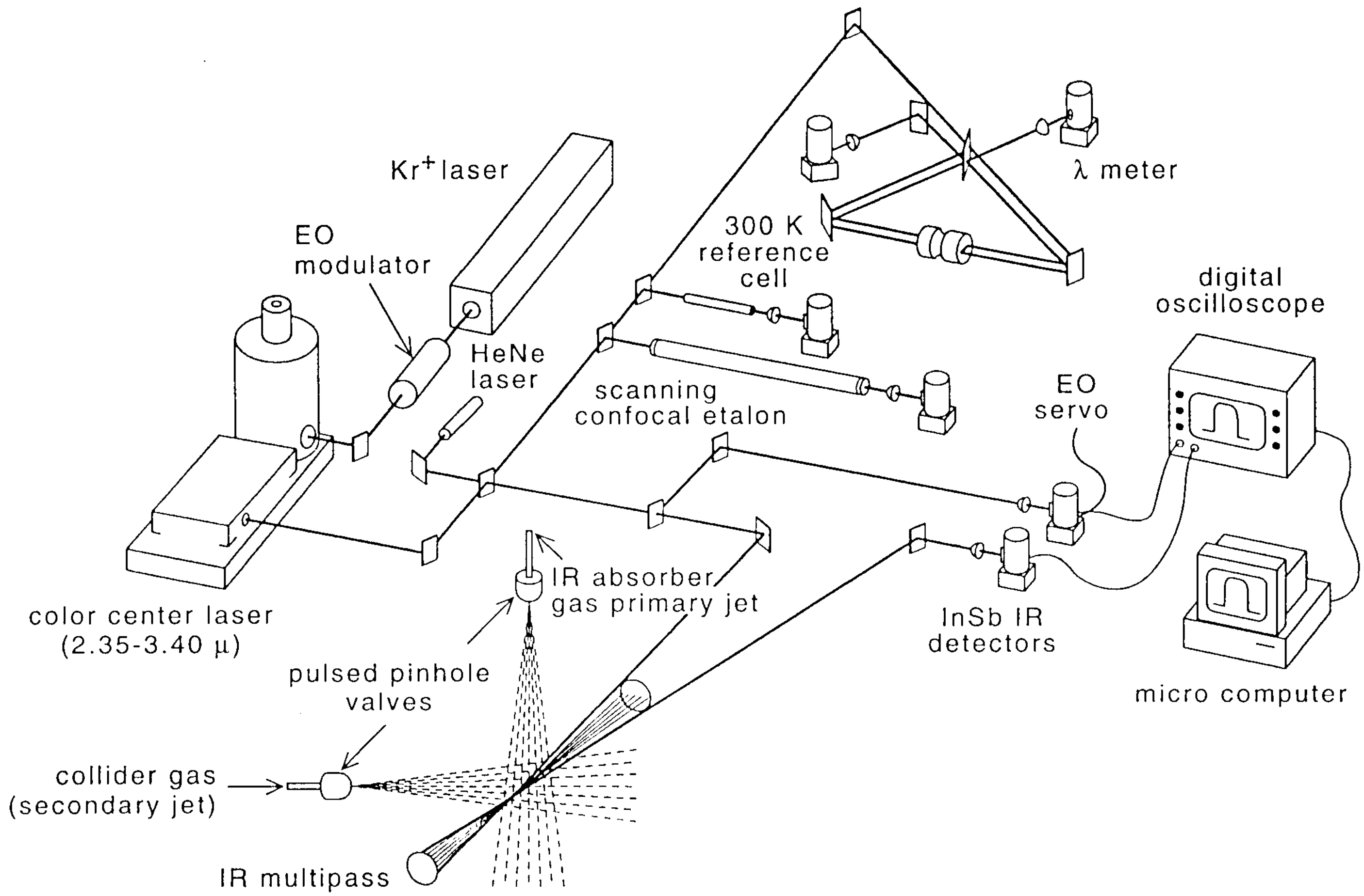

Fig 2.1: Schematic of IR spectrometer and crossed jets experiment.

when aligning the high reflector and output coupling mirrors. A (room temperature) tube pressure of about 150 mTorr is recommended by the manufacturer and proves to correspond roughly to minimum noise and stable operation. The supplied Hastings gauge, which monitors the laser tube pressure via the ballast volume, may be read (with the laser off!) with one of the ubiquitous Varian 801 meters and interpreted using the calibration curve below which was determined by comparisons with a calibrated Hastings meter borrowed from the research group of Dr. J. Hall. (Fig. 2.2).

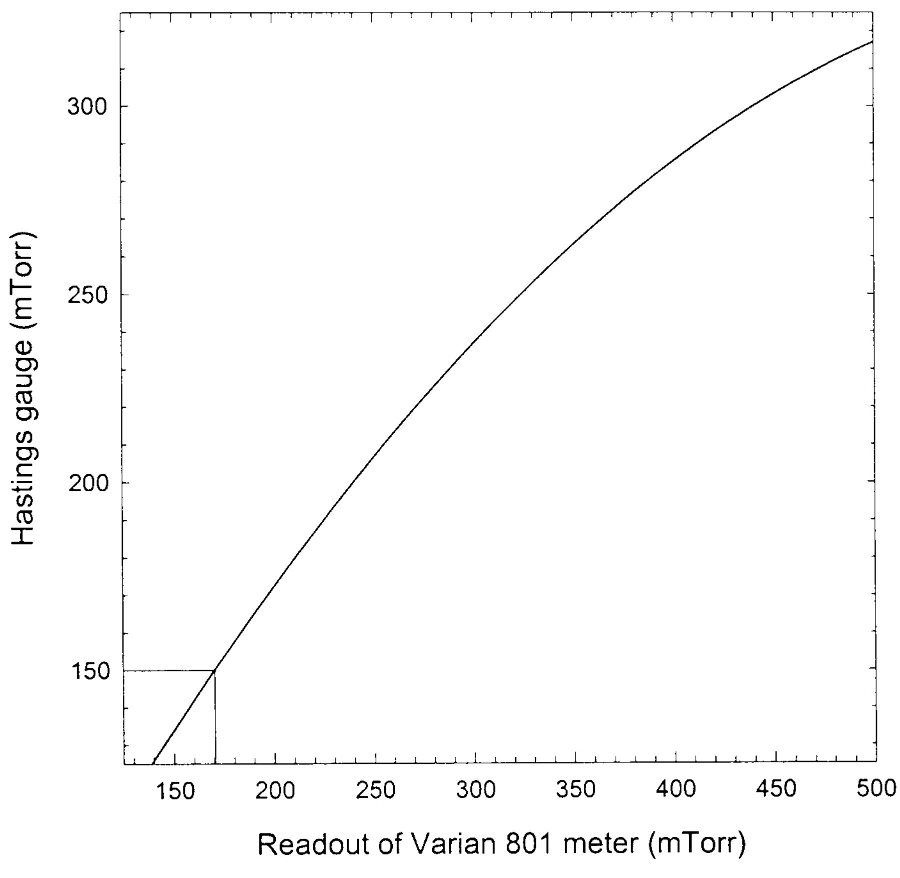

Fig. 2.2: Calibration curve for converting Varian 801 reading of Kr ion laser Hastings gauge to actual pressure.

Thus a normal operating pressure of 150 mTorr reads about 170 mTorr on the 801 meter. Pressure decreases with normal use of the laser and must be maintained by periodic manual addition of Kr gas—*there is no operational autofilling function in this system*. Aliquots of Kr gas are added to the laser tube using a home built switch to open two solenoids valves. The switch circuit (Fig. 2.3), is connected to wall AC power and to three banana plugs inside the laser head according to color code.

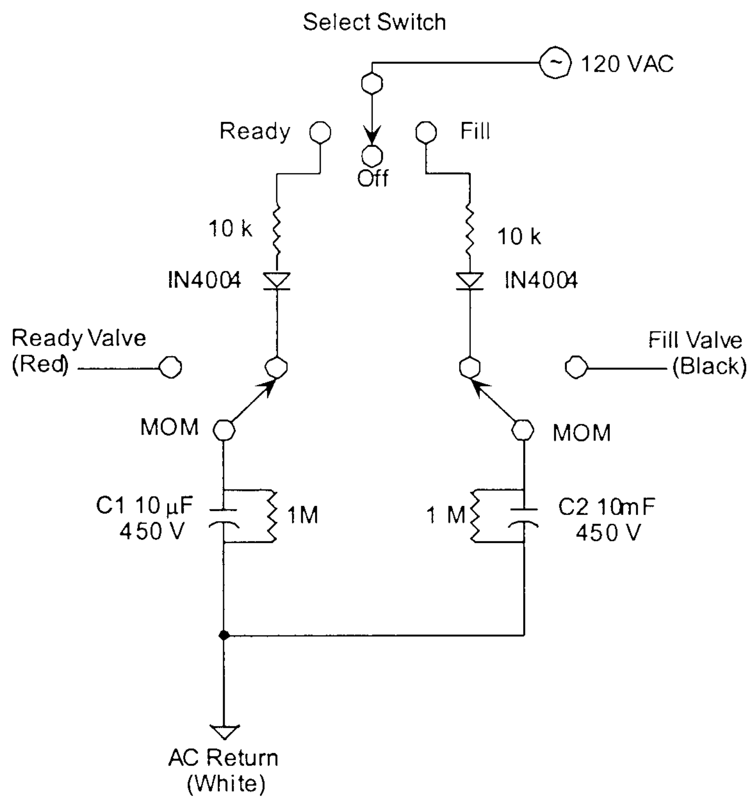

Fig. 2.3: Circuit diagram for manual krypton fill box.

A three position switch selectively charges capacitor C1, neither, or C2. Two momentary switches are used to individually discharge the capacitors through the solenoid valves (simultaneously disconnecting the capacitor from the charging current). The fill box should be operated as follows to ensure that only single aliquots are added at a time.

First the select switch is set to "Ready", then the individual ready momentary switch is pushed to discharge C1 through the first solenoid. This fills the small aliquot volume (~10–20 ml) with fresh Kr gas from the high pressure reservoir. The select switch is then set to "Fill" and the fill momentary switch is pushed, discharging C2 through the second solenoid, releasing the high pressure aliquot into the tube + ballast volume. Setting the select switch to the middle "Off" position leaves both capacitors disconnected from charging current, allowing them to drain via resistors to ground. Power supply passbank voltage for given request current should increase by ~2V per Kr aliquot.

Slightly higher tube pressures (up to ~200mTorr) result in reduced output power but are not damaging although ultimately, at even higher pressures (≳400 mTorr), the discharge will not strike and the laser will fail. If this occurs, the laser may be recovered by pumping out some of the Krypton gas from the ballast tank through a clean, liquid nitrogen (LN_2) trapped pumping system. Subsequent warming of the cold trap should be done, as always, with the vacuum pump running, as some solid Kr may accumulate in the trap. Severe amplitude noise arises from low tube pressure which can also promote ion impact damage to the cathode. An operational rule of thumb is to check the tube pressure daily, but also anytime the laser displays abnormal behavior. Also useful for "diagnosis at a glance" is this relation which holds for moderate changes in tube pressure: For given laser tube current, *increasing* passbank voltage indicates *decreasing* tube pressure, and vice versa.

Passbank voltage, indicated along with discharge current on the power supply front panel, must be >10 V for active current stabilization but should be kept below ~35 V during typical operation to maximize lifetime of passbank transistors and Zener diodes. Once the correct tube pressure is achieved, the preferred range of passbank voltage can be obtained by resetting the taps of the main power supply transformer. Instructions (but not the above stated motivation) for setting the transformer taps are in the laser manual. Typical single line (647.1 nm) TEM_{00} output is ≥2 W at 40 A of tube current, increasing to ~3 W at maximum currents of 60–65 A. Operation on all red lines (with wavelength selecting prism removed) yields ≥5 W maximum power.

A slow flow of clean N_2 flows through the volume between the Brewster windows and end mirrors to reduce the accumulation of burned-on contaminants. Nevertheless periodic cleaning is required. The wavelength selecting prism, high reflector, and output coupler, can all be removed from the laser head in their bayonet mounts and cleaned effectively with twice distilled spectral grade methanol available from the Special Techniques shop at JILA. Brewster windows can be similarly cleaned, but occasionally (~ once per year) require cleaning with a solution of 2–3% ammonium bifluoride (ABF) in distilled water. This caustic solution should be kept from human surfaces. The procedure for cleaning is to scrub the window for a few seconds with a clean cotton tipped swab dipped in the ABF solution. The solution is then washed *completely* from the window using more swabs dipped in pure distilled water. Final cleaning is with twice distilled spectral grade methanol. Safety note: many of the components inside the laser head are biased at ~400–600 V *whenever the power supply is on* (whether or not the "start" button has been pushed). In addition, some components, such as the Hastings gauge on the Kr ballast tank, take a long time to discharge. Probe with a DVM before probing with fingers!

2.3 F-center laser

Typically 1.5–2.0 W of 647.1nm light from the Kr ion laser is first attenuated to 700 mW–1.2 W with an external EO modulator, described below, then steered through the FCL input alignment irises. This red light is used to optically pump the

LN_2 cooled lithium doped alkali halide crystals, KCl (#2) and RbCl (#3) which comprise the laser media of the FCL. Crystal #1, KCl doped with sodium, slightly extends the short wavelength range of the laser but cannot be pumped with red Kr ion laser lines and is not used. Pump power should be limited to <1 W for crystal #3 and <2 W for crystal #2, as explained in the FCL manual.

The laser cavity is formed by a high reflecting mirror and an adjustable grating which output couples in zeroth order, retroreflects in first order, and serves as the coarse tuning element (Fig. 2.4). A single longitudinal mode is selected with an intracavity etalon, the spacing of which is tuned with a piezoelectric translator (PZT). The manufacturer supplied PZT for scanning the cavity high reflector has been disabled and broader continuous tuning is achieved with a pair of CaF_2 plates mounted at ± Brewster's angle in the cavity. These plates are counterrotated through small angles with galvo drivers to vary the optical path length of the cavity.[1] Rotation of ≤2 degrees tunes the laser frequency over 0.8 cm^{-1}, a range that greatly exceeds the continuous tuning requirements of the present experiments.

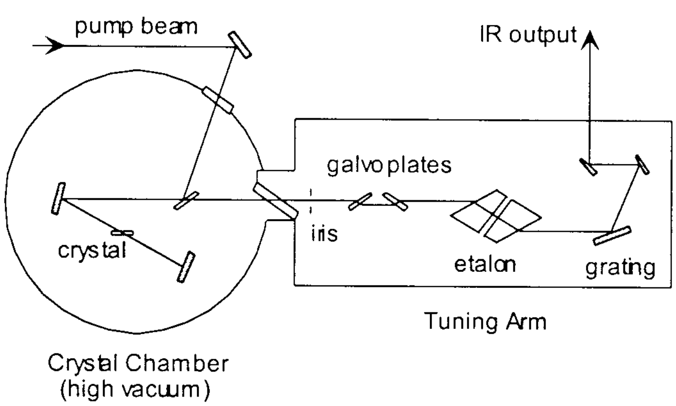

Fig. 2.4: Schematic of modified Burleigh F-center laser.

To maintain the same resonator mode, the etalon spacing must be scanned synchronously with the galvo plates. This is achieved by supplying to the etalon PZT, a feed-forward voltage proportional to the galvo current. Further, a servo loop is employed to lock the etalon spacing to the transmission maximum. The PZT mounted etalon is dithered over a small fraction of its travel corresponding to ~1/10 the etalon FSR. This results in a small-amplitude modulation of the IR light at the 2 kHz dither frequency which is recovered with phase-sensitive detection through a high-Q synchronous digital filter. At present, the IR power modulation is actually suppressed by the EO-based intensity servo described below. Therefore, the modulation signal is recovered (only with the "AUTO" mode activated), from the visible photodiode in the EO head, which senses the Kr^{+} laser intensity. This signal is then demodulated to generate a correction voltage which is sent to the etalon driver. Single mode scanning is thus made robust against thermal drift, vibration, PZT drift and small mismatch of the galvo and etalon scan rates. The galvo driver and etalon servo circuitry are the designs of Dr. Jan Hall and were originally developed for the JILA ring dye laser.

The synchronous filter output from the etalon servo box also provides a useful diagnostic of the FCL cavity alignment. Adjusting the etalon voltage with the servo lock off, one should see a rectified sine wave output that changes sign as the etalon scans from one side to the other of the transmission maximum. (See Fig. 2.5)
If the amplitudes of the positive and negative signals are unequal, then the etalon is misaligned and the servo will not reliably maintain a single-mode scan. Most often, in this case, the etalon is misaligned in the tuning arm and can be corrected with small adjustments of the etalon position. Proper alignment is also checked by "mode hop" scanning the laser. Ramping only the etalon voltage, the laser jumps to adjacent etalon-allowed longitudinal modes. About 9-10 V should be required to hop modes. If proper alignment cannot be obtained by adjustment of the etalon position in the

tuning arm, then the etalon may be misaligned internally. In this case, the etalon should be removed from the laser and aligned with a collimated HeNe laser beam according to the procedure documented in the FCL manual.

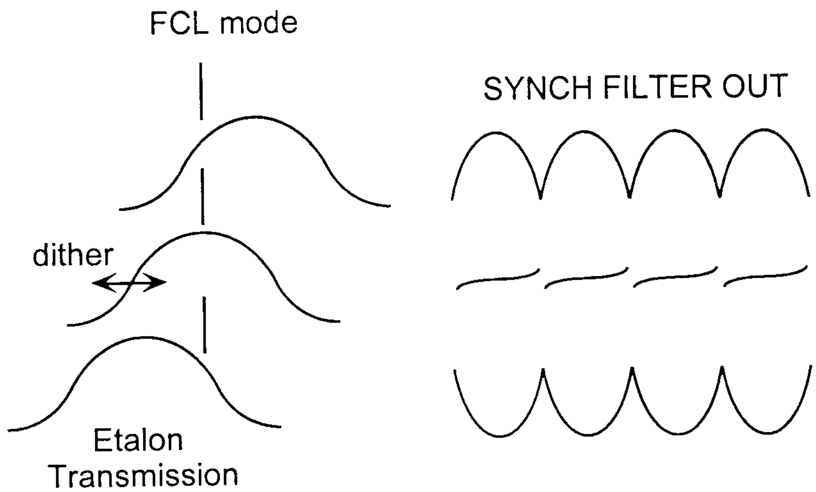

Fig. 2.5: Synchronous filter output from the FCL etalon servo. Scanning the etalon spacing from one side of the transmission maximum to the other changes the sign of the rectified sine wave output. At the transmission maximum, the minimized intensity modulation is at twice the dither frequency and the rectified signal integrates to zero. Imbalance in the signals on opposite sides of the transmission maximum indicates misalignment of the laser cavity.

2.4 IR diagnostics

The horizontally polarized output of the FCL is split into several beams for diagnostics and signal detection. Frequency of the FCL output is measured with a traveling Michelson interferometer "λ-meter" after the design of Hall and Lee.[2] A practical discussion of the λ-meter, including a tutorial for its alignment, is given in Ref. 3.

Briefly, a portion of the IR beam and overlapped output from a frequency stabilized HeNe laser[3] is split and the two branches are directed to back-to-back corner cubes mounted on a cart that travels on an air bearing. The IR and visible frequencies of the separate branches are thus Doppler shifted in opposite senses. The beams are recombined on a beamsplitter and monitored on separate IR and visible detectors. Intensities of the recombined beams are modulated at the difference frequencies ($\Delta\nu$) arising from the Doppler shifts, which are proportional to the laser frequencies and the cart speed. The IR frequency is recovered from

$$\nu_{IR} = \frac{\Delta\nu_{\mathrm{IR}}}{\Delta\nu_{\mathrm{vis}}}\nu_{\mathrm{vis}} \tag{2.1}$$

where ν_{vis} is the known, stabilized HeNe frequency. The difference frequencies are measured in a discriminator and their ratio is determined by counting the number of IR zero crossings occurring in a preset number (~10^5) of HeNe zero crossings. Phase-locked multiplication of the IR frequency before discrimination increases the counting precision which is limited to integer ratios; the resulting precision is ~ 0.0005 cm^{-1}. As a further check, absolute frequencies can be obtained from molecular transitions in a low pressure sample cell. Output from the λ-meter IR detector also provides a good indicator of single mode operation of the FCL since multimode output causes low frequency amplitude modulation of the interference fringes.

Another portion of the IR light is sent to a home-built scanning confocal Fabry Perot interferometer (FPI), which serves as both low-resolution spectrum analyzer and marker cavity. The two mirrors comprising the cavity are separated by a Pyrex tube which has been ground at one end to provide a flat surface perpendicular to the tube axis, and flared at the other end to a diameter slightly greater than that of the mirror. A hollow, cylindrical PZT is cemented to the ground end of the tube and one mirror is then cemented to the PZT. With the tube held in adjustable mounts, the overlapped HeNe and IR beams are aimed down the center of the tube which is then adjusted to retroreflect the visible beam. The second mirror, held in an adjustable mount, is then placed in the flared end of the Pyrex tube, centered on the input beam, and adjusted to retroreflect the HeNe tracer from the back of the mirror. This brings the arrangement close to concentric alignment, in which the cavity behaves as a "flat-flat" etalon with a free spectral range (FSR) of c/2L, where L is the cavity length and c is the speed of light.

Final alignment is performed while scanning the cavity length by applying a 30 Hz sawtooth voltage ramp (~400 V) to the PZT. Transmission fringes should be visible on an IR detector at this point. The second mirror is adjusted for maximum finesse and then cemented in place. The aligned FPI may now be translated off-axis to achieve the "bow-tie" configuration of reflections in the cavity. This reduces the FSR to c/4L and hence, the finesse is reduced 2 fold, but is necessary to avoid troublesome optical feedback of the IR light. The voltage ramp amplitude is usually adjusted so that two interference fringes appear in each cycle, so that additional unwanted laser modes are seen as extra peaks between the primary fringes.

Time delay from the beginning of each sawtooth cycle to the appearance of the first transmission fringe varies continuously as the IR laser frequency is scanned and is stored as a voltage via time-to-amplitude conversion (TAC), in an integrator plus sample-and-hold circuit designed by Dr. Eberhard Riedle. A linear frequency scan generates a uniform sawtooth output from the TAC providing frequency markers separated by the off-axis cavity FSR of 151 MHz. Laser mode hops appear as discontinuities in the TAC output which is stored as part of the data record.

2.5 IR absorption detection

A matched pair of LN_2 cooled, low noise (<2 pA $Hz^{-1/2}$) InSb infrared detector/amplifiers (Cincinnati Electronics, SDD-1963-S1) are used in the crossed jet experiments, one sensing transient absorption signals and the other providing a reference of the IR intensity. Transimpedence of each internal amplifier is 50 kΩ and is easily modified by changing the feedback resistor. A 4–15 pF capacitor has been added in parallel with the feedback resistor to trim the amplifier frequency response. The detector/amplifier bandwidth is measured with a fast (<3 ns risetime) IR LED to be about 900 kHz with a gain peak of < 0.5 dB at 500 kHz. Figure 2.6 shows the detector frequency response and the effect of adjustments of the trimming capacitor.

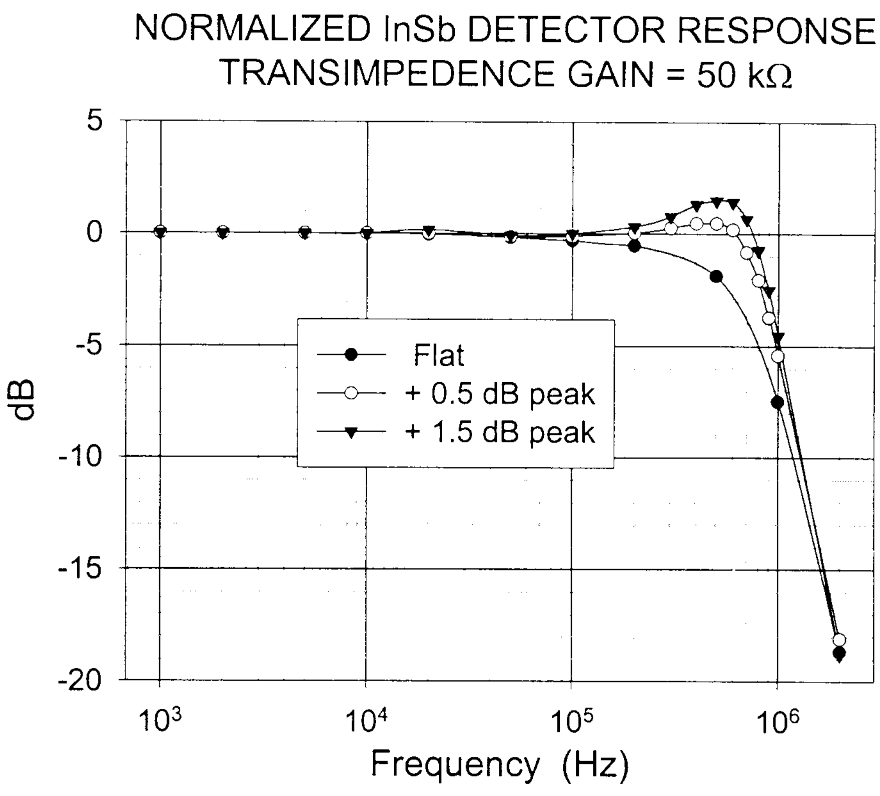

Fig. 2.6: Frequency response of the Cincinnati Electronics, SDD-1963-S1 Infrared detector measured with an OPF345 high speed IR LED. An added trim capacitor (4-15 pF) is used to select best gain response and bandwidth characteristics.

A portion of the IR laser beam is split nearly equally and steered onto the signal and reference detectors. Detector output levels are attenuated, balanced electronically and then subtracted in an instrumentation amplifier (Burr Brown INA110), providing signal output with high rejection of common mode noise. Buffered DC output of the signal detector is also stored via A/D acquisition allowing transient absorption signals, averaged in a transient digitizer or digital storage oscilloscope, to be recorded in absolute absorbance units. Although with some effort the dual beam subtraction can reduce the common mode noise in a limited bandwidth to nearly the shot-noise limit, the balance of the two channels is very critical and must be manually adjusted frequently. Furthermore, signal subtraction does not adequately cancel low frequency noise ($\leq$100 Hz).

This situation is substantially improved by a second noise suppression scheme shown in Fig. 2.7. Buffered DC output from the reference InSb detector is used as feedback in an active proportional-integral-differential servo loop which modulates the intensity of the Kr^+ pump laser light with a fast (5 MHz) EO modulator in the beam path. The control circuitry (Fig. 2.8), designed and implemented by Terry Brown at JILA, employs two integrators, which aggressively cancel low frequency noise, and proportional and differential gain stages to provide stability and greater servo bandwidth. Two modes of operation are selectable from the front panel of the control box. In "Kr" mode, output from a visible photodiode which monitors a portion of the Kr^+ laser light split-off after the EO modulator, is used in the feedback loop to stabilize the transmitted intensity. Already, in this mode, noise on the IR light is reduced and the F-center crystals are protected from drift in the Kr^+ laser power. Switched to "AUTO" mode, the servo responds to noise on the IR light sensed at the reference InSb detector and, via the EO modulator, effectively writes "antinoise" onto the pump laser intensity.

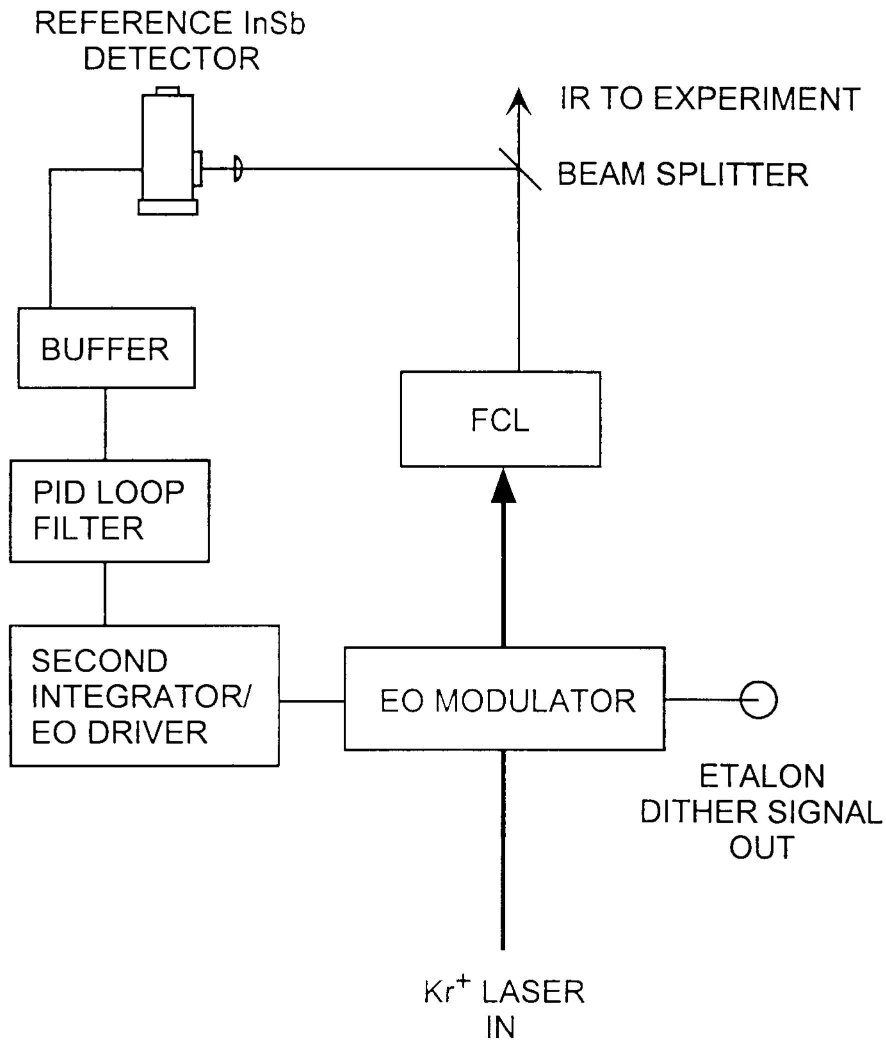

Fig. 2.7: Schematic of EO modulator FCL intensity servo. IR fluctuations sensed at the reference InSb detector are canceled by rapidly varying attenuation of the visible pump laser intensity.

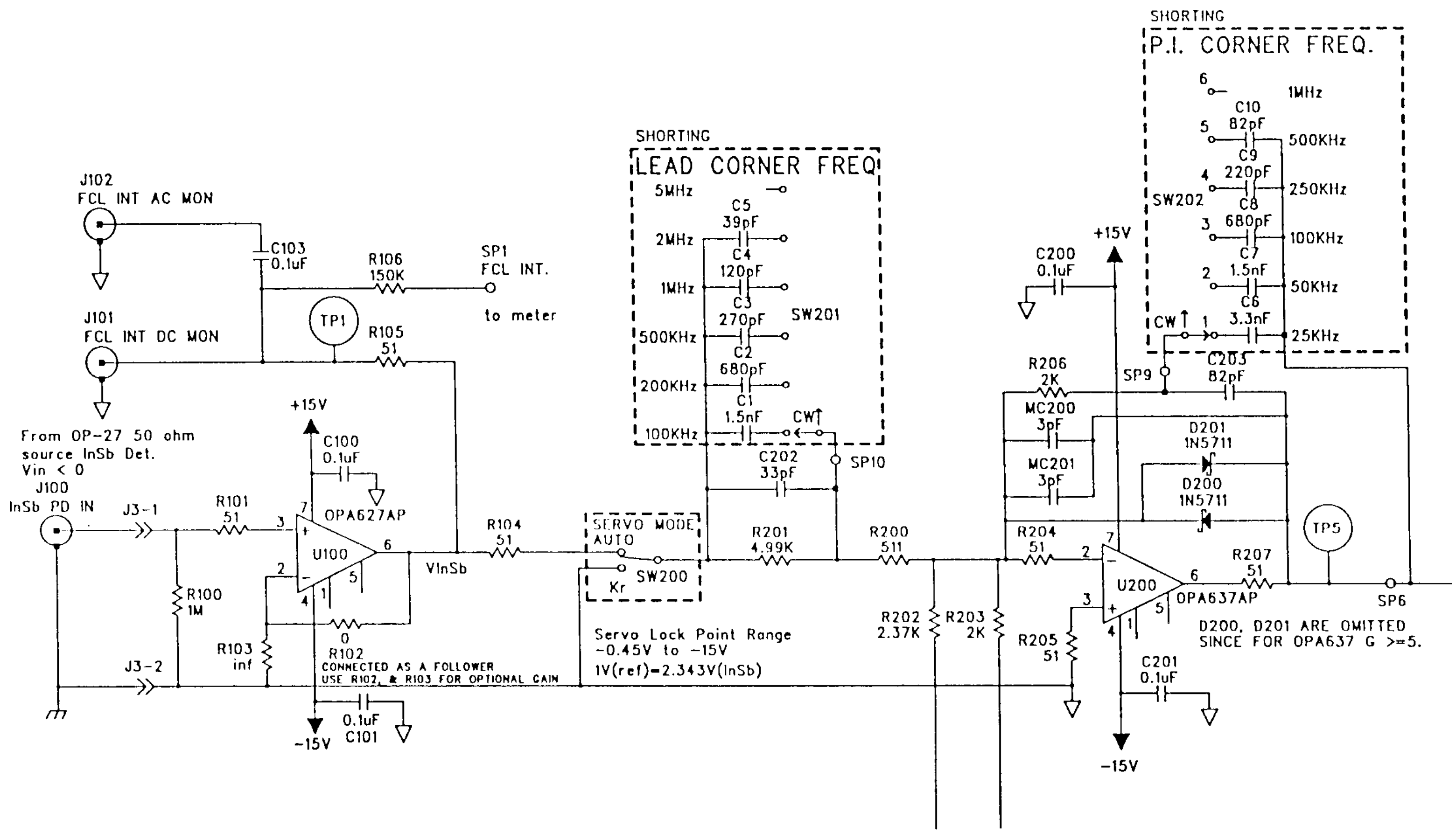

Fig. 2.8: Circuit diagram for FCL intensity servo (Part 1 of 3)

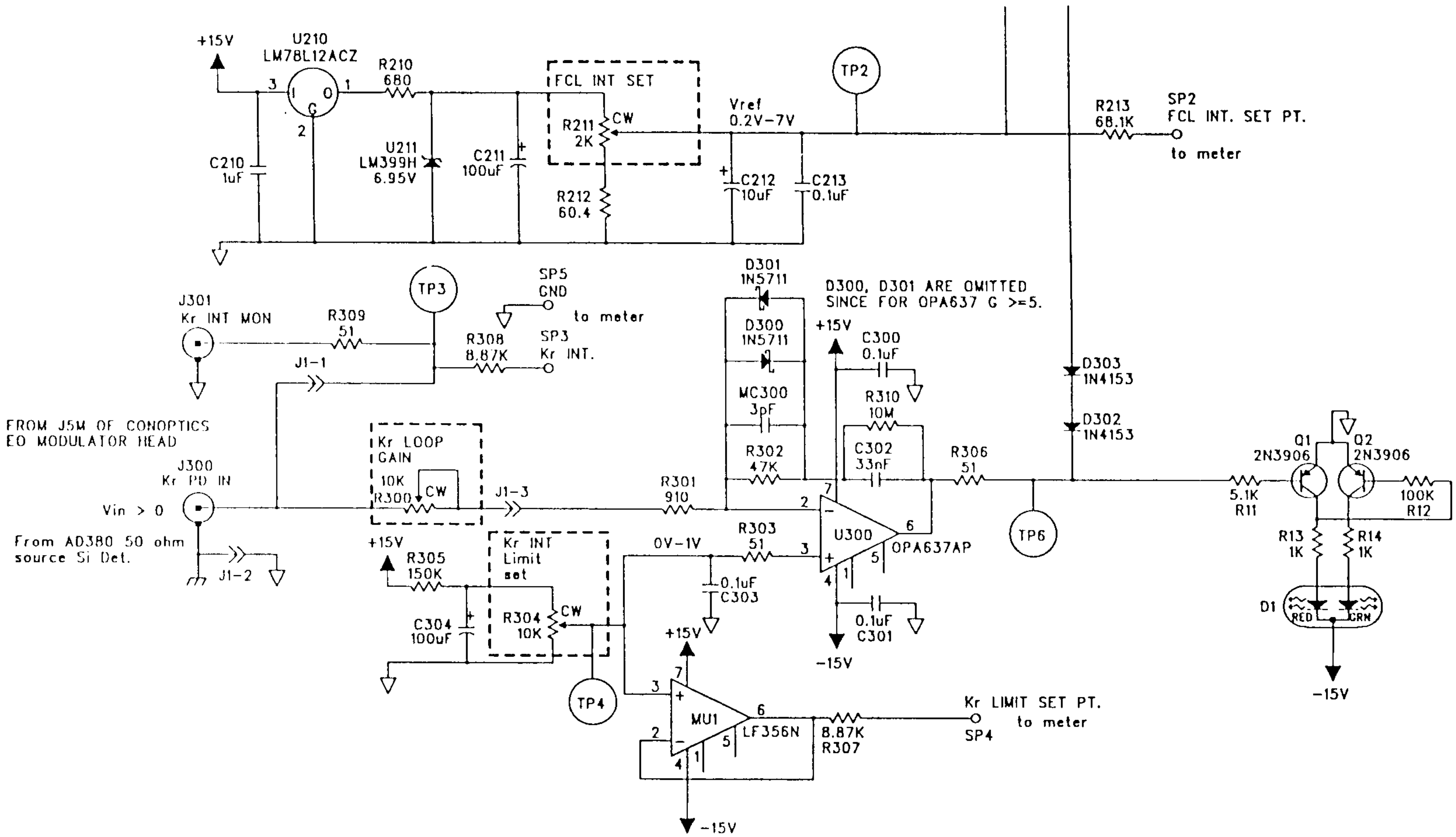

Fig. 2.8: Circuit diagram for FCL intensity servo. (Part 2 of 3)

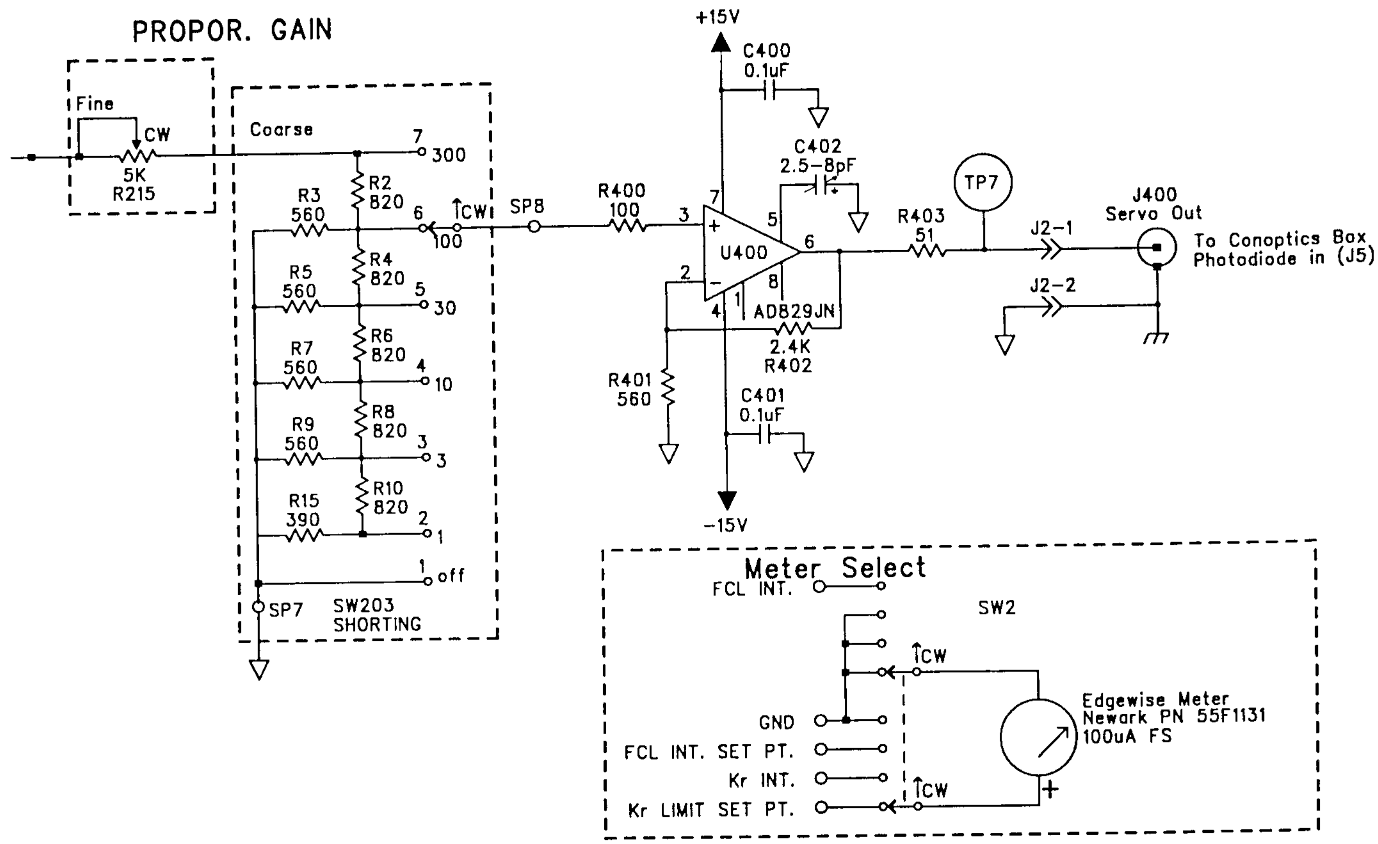

Fig. 2.8: Circuit diagram for FCL intensity servo. (Part 3 of 3)

The benefits of this system are fourfold. First, the noise suppression does not depend on the balance of signal and reference detector levels and hence vastly reduces the effort expended optimizing signal/noise during routine laser scans. Second, the DC coupling and double integration in the loop filter greatly improve cancellation of low frequency noise which often survives the AC coupled signal subtraction. Third, the servo loop stabilization reduces IR amplitude noise at *all* points providing cleaner lambda-meter fringes and quieter FPI transmission peaks. Finally, the compact (5"×2$^{1}/_{4}$"×7") control box is placed for convenient access and allows facile control of the pump laser intensity which is especially useful when tuning the FCL broadly over the crystal gain profile, or when switching between laser crystals. Protection circuitry prohibits the servo from driving the pump laser intensity above a user determined limit.

Proportional gain is adjusted on the back panel for best performance by the following method. A small (~10 mV) square wave is sent to the external input found on the back of the EO driver, resulting in square wave modulation of the pump laser and IR laser amplitudes. With the "InSb" mode selected, the servo attempts to cancel this modulation. Gain is adjusted to null the square wave function observed at the InSb detector with the fastest settling time but without ringing. Figure 2.9 shows the signal at the reference InSb detector when the loop filter gain is (a) too low, (b) optimum, and (c) too high. Under this latter condition, the servo is marginally stable and may oscillate.

To operate the system, first the servo mode is set to "Kr" and, with a power meter in the Kr^{+} laser beam path, transmitted intensity is adjusted with the "Kr INT. LIMIT SET" knob to a desired level safe for the F-center crystal. The FCL may now be pumped and all the typical beam alignment procedures are carried out in this mode. With IR light on the reference detector, the servo is next switched to "AUTO".

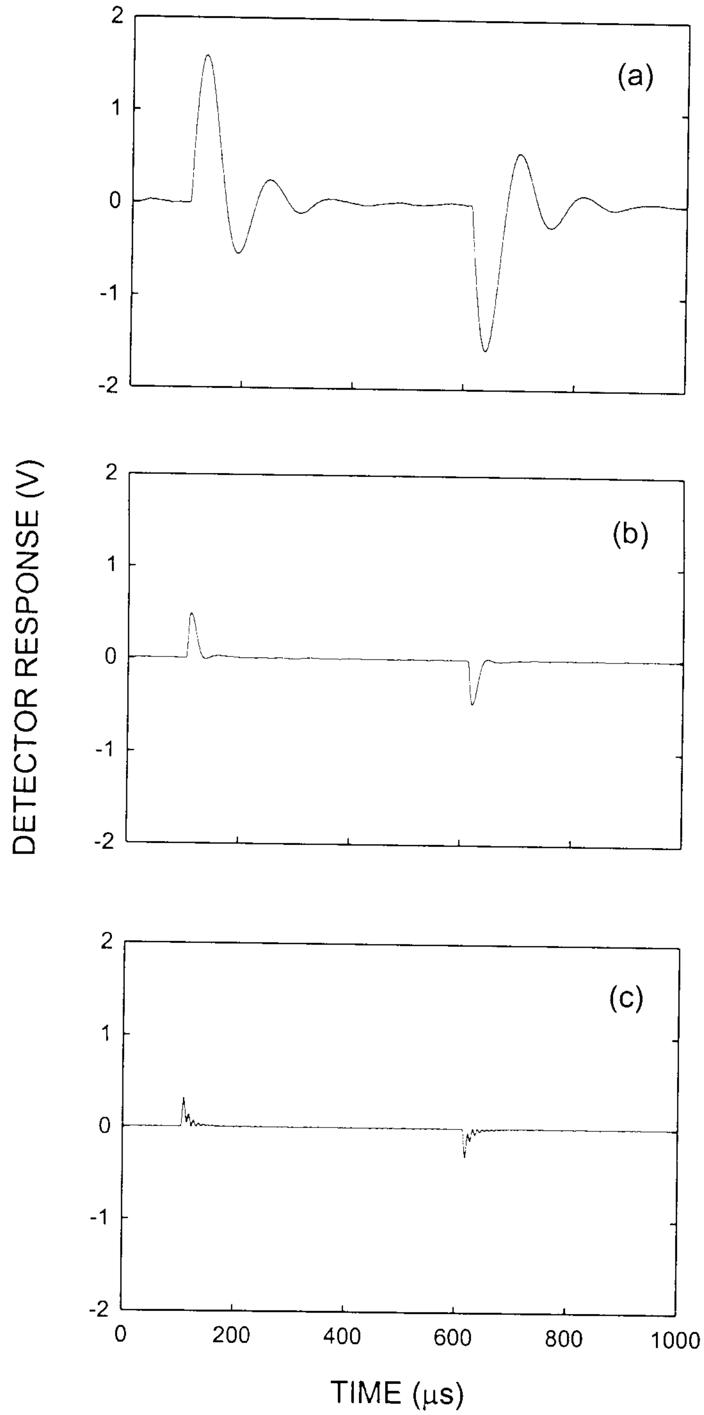

Fig. 2.9: Reference detector output with square wave modulation of the Kr^{+} laser intensity. Proportional gain of the FCL intensity servo is adjusted to achieve maximum cancellation of intensity modulation without ringing. (a): Gain is too low. (b): Optimum gain. (c): Gain is too high, servo may oscillate. (See text for details.)

A red/green LED indicates the active stabilization mode. If this indicator remains red, then the requested pump laser intensity is above the limit set in the first step. In this case the "FCL INT. SET" knob is turned counterclockwise until the indicator turns green. This lowers the voltage setpoint level from the InSb detector *that the servo will try to maintain*. The resulting pump laser power level is observed on the front panel meter with the selector switch set to "Kr INT." The servo is now actively stabilizing the IR intensity. If the IR beam is interrupted, the circuitry automatically switches to "Kr" mode and will recover when the beam is unblocked.

The servo loop gain rolls off at higher frequencies, and signal subtraction contributes to noise suppression above about 25 kHz. Of course, *incoherent* noise on the signal detector cannot be suppressed by either feedback on the reference detector output, or by dual beam subtraction. With careful alignment and clean optics, incoherent noise is minimized and the system detection efficiency is better than $3 \times 10^{-7}/\sqrt{\text{Hz}}$ over the full detector bandwidth.

2.6 Nitrogen purge system

For operation at frequencies near atmospheric water absorptions, the entire IR spectrometer is enclosed in a Plexiglas case with removable lids. This ~400 liter volume is purged by the dry nitrogen exhaust of the LN_2 cryotrap of the vacuum chamber diffusion pump. The cold nitrogen gas is warmed to room temperature in a 50 foot coil of copper tubing placed under the diffusion pump before entering the purge box through several inlets tubes. One inlet tube is attached to a hypodermic needle which fits into a small hole in the Pyrex tube of the scanning FPI for quick purging of the cavity. Overall flow rate is controlled by the LN_2 flow into the trap, and flow to individual tubes is controlled with needle valves. For further purity, air floating the λ-meter cart is replaced with dry nitrogen from a 1A cylinder.

Of course all this effort is wasted if the FCL tuning arm is full of room air. This volume may be purged with a slow flow of dry N_2 through inlet and outlet valves on the tuning arm cover flange. For operation near strong atmospheric water absorption however, the tuning arm must be evacuated. For this purpose a one inch diameter pump-out port fits onto the cover flange and connects to a LN_2 trapped mechanical pump. High voltage to the etalon must be turned off during pump-down to avoid arcing in the etalon PZT stacks. These electrode and PZT crystal assemblies are *epoxied* together resulting in many low conductance gas pathways (virtual leaks). It is therefore necessary to maintain the tuning arm pressure below a few mTorr for ~6 hours before applying full voltage to the etalon. Also during pump-down, some misalignment of the laser cavity occurs which is compensated for primarily by adjusting the grating tilt. A butterfly valve in the fore line may be used to pump out the tuning arm in aliquots so the alignment can be adjusted in stages to maintain laser output. This prevents the irritation of trying to align the pumped-out laser with no signal to look at.

2.7 Crossed jets chamber

The vacuum chamber used in the crossed jet experiments described in Chapters 5–8 is a 65 liter cube constructed from 3 cm thick aluminum. Five of the cube faces are cut out leaving 5 cm borders with machined O ring grooves and tapped holes for attachment of 3 cm thick square Plexiglas flanges. Multipass optics, IR windows, pulsed valves, vacuum gauges, and other diagnostic equipment and feedthroughs are held on smaller aluminum or stainless steel flanges mounted on these Plexiglas sides. The bottom of the cube is machined to mate to a floor mounted table which suspends a 6000L/s 10-inch oil diffusion pump backed by a remote Roots blower and rotary vane pump combination. The diffusion pump is separated from the chamber by a LN_2 cooled baffle to reduce oil backstreaming into the chamber. Base chamber pressure with no valves operating is ~1×10^{-6} Torr (1 Torr = 133 Pa). Pulsed jet sources described below are held in the chamber in rigid mounts which may be positioned to various angles and separation distances. Gases are supplied to the jets via stainless steel feed tubes passing through O ring vacuum seals. Outside the chamber, the feed tubes connect to a stainless steel gas manifold with attached capacitance manometers for monitoring stagnation pressures in the plenum volumes of the valves. The gas manifold includes a valved connection to the Roots blower/mechanical pump station allowing for rapid evacuation of the manifold and/or the pulsed valves.

Infrared light from the FCL overlapped with the visible HeNe tracer beam enters the chamber through a CaF_2 window and is multipassed in an optical cell, similar to the design by Herriot,[4] 16–22 times through the jet intersection region at angles nearly orthogonal (± 3°) to the collision plane defined by the two jets. The signal beam then exits the chamber through the same window and is collimated and focused onto the signal detector with a pair of CaF_2 lenses (f=50.0 and 2.5 cm). An equal portion is sent to a matched reference InSb detector for rejection of common mode laser noise as mentioned above.

The multipass cell is formed by two identical spherical mirrors positioned at slightly less than the spherical spacing of twice the radius of curvature of the mirrors. The IR beam is brought to a focus at the center of the multipass cell with a CaF_2 lens placed just outside the cell. In our implementation, which is borrowed from Perry[5], the beam enters the cell under one of the mirrors and off center and is steered diagonally to the upper opposite position on the second mirror. The second mirror is then adjusted to reflect the beam back to the first mirror just above the input beam. From there, small adjustments will generate a multipass pattern which is tightly bundled halfway between the mirrors and which forms a pattern of uniform spots in half-ellipses on each mirror (See Fig. 2.10). With clean mirrors the IR intensity loss was measured to be ~15% for 18 passes, corroborating the better than 99% reflectivity of the gold mirrors. In addition to the central focusing feature, this arrangement has the advantage that the beam spots become more separated near the mirror edges. This facilitates getting the laser beam in and out of the cell with minimal clipping.

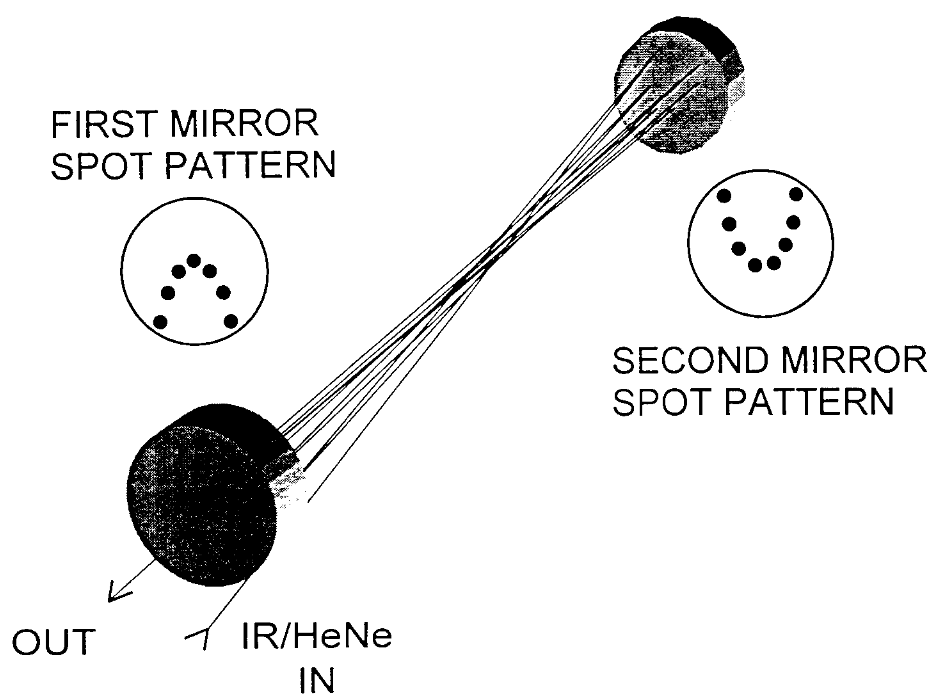

Fig. 2.10: Layout of optical multipass cell for crossed jet experiments.

Annoyingly, our usual tracer HeNe spots are invisible on *clean* multipass mirrors. Alignment of the Herriot cell is thus best achieved with dirty mirrors! Alternatively, a strip of paper can be used to locate spots, or a more powerful (~10 mW cw) HeNe laser beam may be overlapped with the IR beam, affording visible spots on even freshly cleaned mirrors. Irises centered and fixed on the input and output beams allow easy recovery of the cell alignment after the mirrors have been removed, cleaned, and replaced.

2.8 Pulsed jet sources

Several types of pulsed valves have been used in the crossed jet experiments. Commercial solenoid activated valves (General Valve, Series 9) are used to generate supersonic pinhole expansions and are conveniently small (1.75 cm dia. × 4.0 cm). The sealing poppets of these valves are subject to wear however, and must frequently be replaced to ensure consistent, reproducible gas pulses. The driver used for these valves is a home-built current pulse generator described elsewhere.[3] Adjustment of these valves is accomplished by tightening the aperture cap onto the threaded valve body. Pulse duration is varied by adjusting the current pulse duration but the minimum for a fully opening valve is ~800 μs FWHM.

A larger (6.85 cm dia. × 6.5 cm) but faster and more reliable source is based on the design of Proch and Trickl.[6] This valve is opened with a PZT disk available from Physik Instrumente (Model P-286.27), and seals with a Viton O ring around the pinhole aperture. Fig. 2.11 shows a simplified cross sectional view of the PZT valve. The sealing O ring, labeled (1) in the figure, is captured on a titanium shaft (2), which is threaded through the center of the PZT disc (3). The disc is supported around its outer edge on a Viton O ring in the valve faceplate (4). Adjustment of the valve is primarily done with the threaded shaft which determines the pressure on the sealing O ring. The valve has proven capable of generating reproducible pulses for many months of daily operation and is thus worth the initial set-up time.

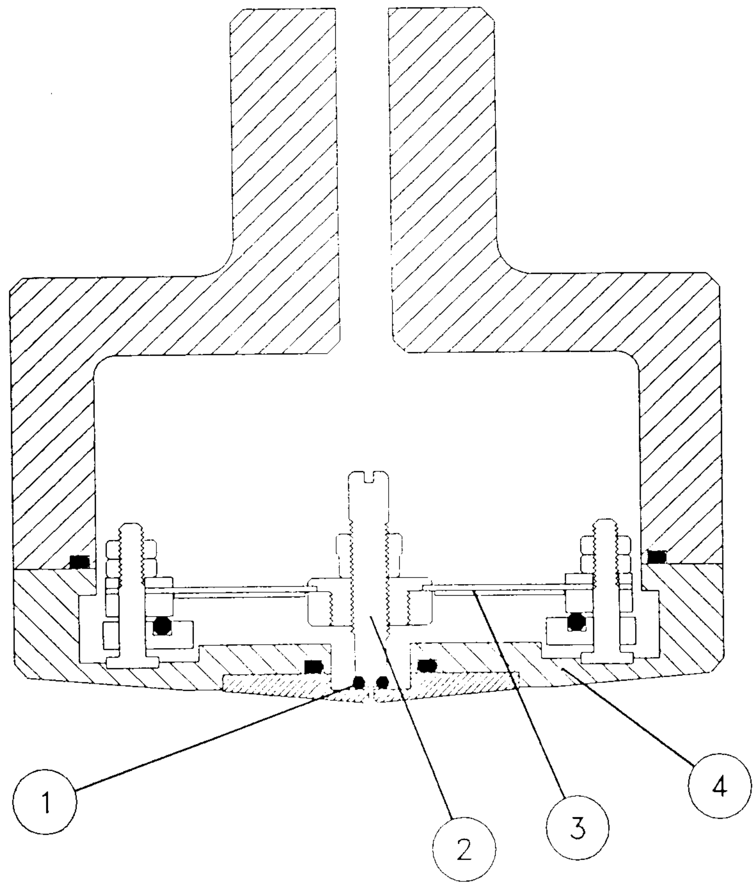

Fig. 2.11: Schematic of PZT pulsed valve after the design of Proch and Trickl, (Ref. 6). A Viton O ring (1) seals the valve aperture and is captured on a shaft (2) which is pulled back when high voltage is applied to the PZT disc (3). The valve mechanism is held on the face plate (4), which can be removed from the valve body and operated independently.

To adjust the valve, first the central shaft and tensioning screws are tightened enough to seal the aperture. This can be confirmed by overpressuring the valve with N_2 and leak checking the nozzle. Next, the back of the valve is removed and the front part is mounted against an O ring seal, to a mating flange kept in B214, which bolts onto the one of the ports of the vacuum chamber. The outside front face of the valve has a ground O ring surface for this purpose. The mating flange also has a feedthrough to hold a hearing-aid microphone attached to a 1/8 inch diameter stainless steel rod. With the chamber pumped out, the valve will let in pulses of room air which may be monitored with the microphone during the adjustment. Leads from the PZT are connected to the HV pulse generator described below taking care to adequately insulate the connections. The PZT cannot withstand HV voltage pulses of the wrong polarity and the leads are color coded: black means negative with respect to red. The *red* lead is therefore connected to the return (HV cable shield), and *negative* pulses are sent to the PZT through the *black* lead.

Optimum valve adjustments differ for very different repetition rates (the valve can operate at up to 3 kHz) so a suitable driver pulse rate is first chosen and an initial pulse width of about 300 μs is selected. Synchronous output signals are available on the driver front panel. Next, the voltage is incremented at the DC power supply until the valve begins to open at about -200 to -400 V. If this fails, the central shaft may be loosened while the valve is running, until the valve opens. After tightening the locknut on the central shaft, the tilt of the PZT disk may be fine tuned using the four mounting nuts around the disk's edge to attain best gas pulse temporal profiles as monitored on the microphone.

The properly adjusted valve opens partially with pulses of ~ -300 V, and opens fully with pulses of about -800 to the rated maximum of -1000 V. To protect the PZT element from excessive force, a minimum rise/fall time of >35 μs is specified by the manufacturer. The risetime is thus limited with a resistor placed in series with the 35 nF capacitance of the PZT disc. Operational caveat: At very low backing pressures (e.g., < 80 Torr for H_2), arcing may occur inside the valve. It is therefore important to switch off the HV pulses before pumping out the valve. Pulse rate and width are varied with controls on the driver described below.

The PZT driver is essentially a HV switch; a circuit diagram is shown in Fig. 2.12. The output rail of this driver is alternately connected to the external HV supply or to ground via two high power FET transistors in a push-pull configuration. Triggering can be selected between internal with adjustable rate or TTL external. The circuit, with integral high voltage storage capacitors, easily switches 800 V, 3.5 A pulses of ~500μs duration. The circuit, with small modifications, is also used to generate HV current pulses for the mini slit discharge source (described in the next section) and the large discharge source in B212. In B241, it is used to quickly turn on a photomultiplier tube immediately following a UV photolysis pulse. It is perhaps worth cautioning that the *transistor cases*, as well as other components on the high voltage side of the circuit, are held at the supply voltage. Careful scrutiny of the circuit diagram reveals this fact, but unfortunately it has also been empirically confirmed.[7]

2.9 Pulsed discharge sources

The reactive scattering experiments described in Chapter 8 require an intense supersonic jet source of fluorine atoms. Several sources were considered for use including continuous flow pyrolysis sources used by other groups.[8,9] However, continuous sources impose greater demand on the vacuum chamber pumping system and in practice, would force an unfortunate trade-off between beam intensity and chamber background pressure. A pulsed pyrolysis source has been described in the literature,[10] but is technologically cumbersome to implement. The simpler solution chosen for this work borrows from the recent invention of a slit aperture pulsed discharge source developed in the Nesbitt group for the purpose of performing spectroscopy on radicals and ions with high sensitivity in a cold supersonic expansion environment.[11]

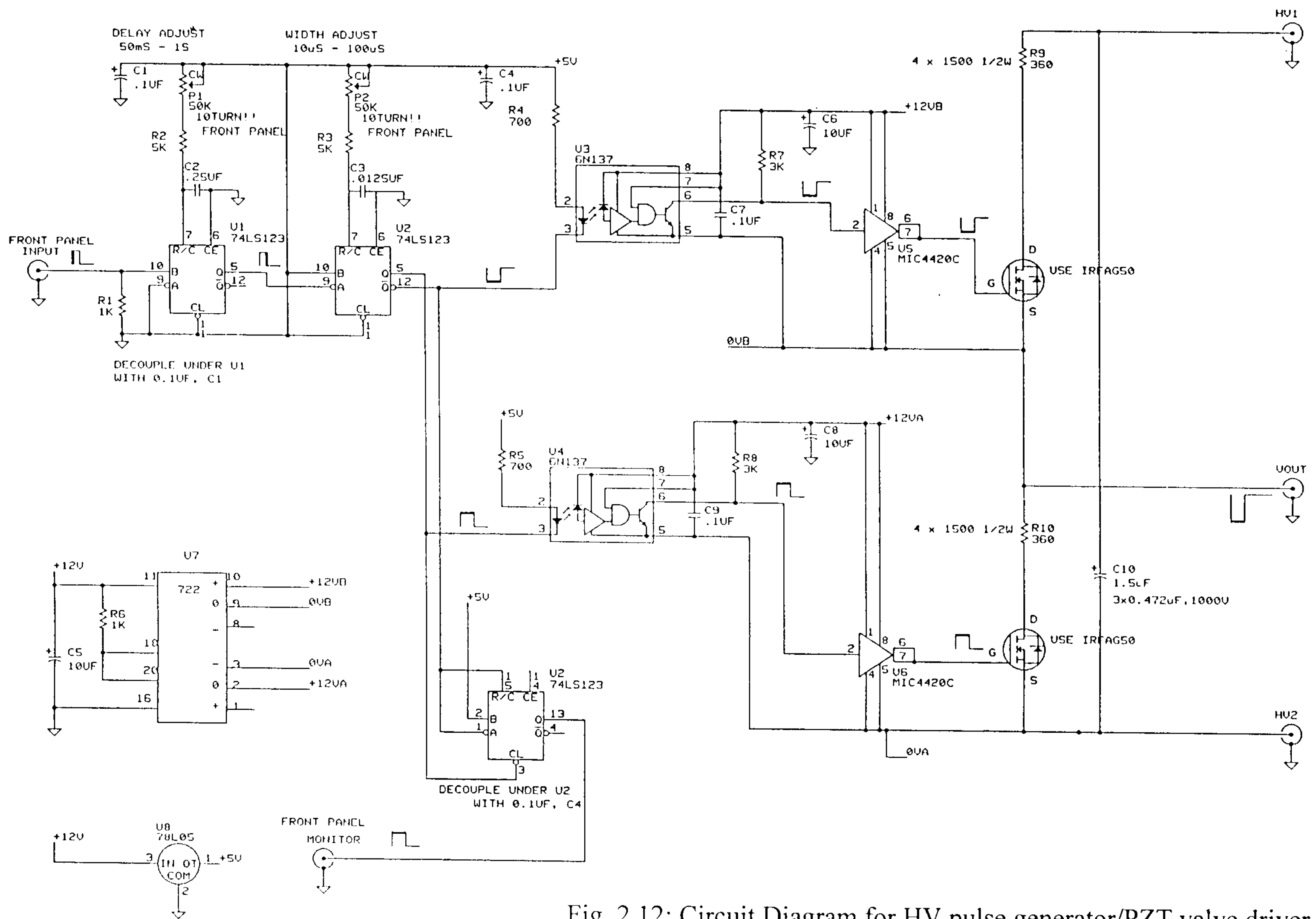

Fig. 2.12: Circuit Diagram for HV pulse generator/PZT valve driver.

The first pulsed discharge F-atom source implemented for the crossed jet experiment was built around a modified commercial solenoid valve (General Valve, Series 9) and consisted of a small electrode with a limiting pinhole aperture, mounted to the valve faceplate with a 0.5–1.0 mm Vespel insulating spacer. With this source and all subsequent refinements, a high voltage pulse (~700 V) biases the electrode negatively with respect to the valve body, resulting in electrons flowing upstream with high mobility in the gas flow. For modest currents, (~10-35 mA for 5% F_2/He) the discharge is completely confined behind the limiting aperture which thus allows species generated in the plasma to be very efficiently cooled in the subsequent supersonic expansion. Also, the short residence time (< 0.5 μs) in the 0.5–1.0 mm discharge region minimizes opportunities for radical-radical recombination. Discharge characteristics vary dramatically with gas mix and to minimize wear of the electrode surfaces; searches for ideal conditions with new gas mixes should be approached from the low current side, increasing the ballast resistance (4kΩ at present) if necessary.

Several modifications were attempted to increase the operating lifetime of the source which tended to fail after several hours of operation due to pitting of the cathode surface. The best solution found to date is essentially a miniature version of the slit discharge source used in the Nesbitt group radical/ion spectroscopy experiments. The miniature slit discharge source is depicted schematically in Fig. 2.13. Slit aperture geometry is similar to the large source, but scaled down ~10 fold. Radiused cathode jaws form the 5.00 mm × 0.300 mm slit separated from the valve body by a 0.50 mm thick Kel-F insulator. Beneath the insulator is a disc of stainless steel shim stock with a 5.0mm × 0.40 mm machined slot which serves as a replaceable anode. Reproducible assembly of the components is accomplished with removable gauge pins, which are placed into alignment holes machined into the

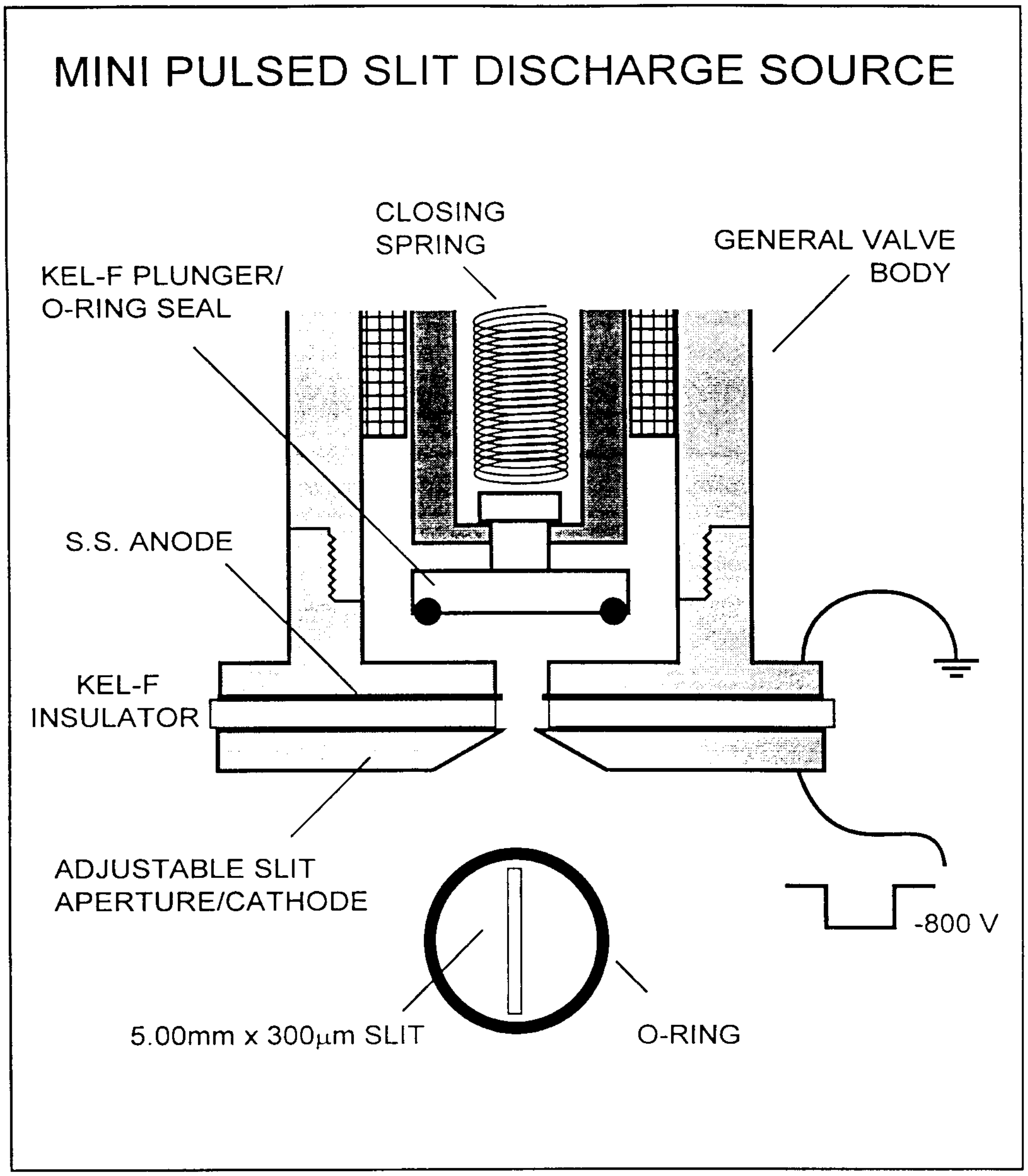

Fig. 2.13: Miniature pulsed slit discharge source used in crossed jet reactive scattering experiments. The slit aperture is sealed by a surrounding O ring which is held in a Kel-F plunger. The plunger is lifted by the modified General Valve armature when a current pulse is applied to the solenoid. A negatively biased, high-voltage pulse applied to the slit jaws during the gas pulse, generates a discharge in the short region defined by a separating Kel-F insulator. Note that this insulator extends slightly beyond the valve diameter to prevent arcing across the outer insulator surface.

faceplate of the valve. The stainless steel anode shim, Kel-F insulator, and slit jaws are placed with their alignment holes fitting over the gauge pins. Alignment holes in the slit jaws are slightly oversized to allow for different slit width adjustments. Nylon screws (they must be insulating!) are placed in six tapped holes and are tightened while the slit jaws are squeezed against the gauge pins to ensure parallel alignment. New nylon screws are used each time the valve is assembled since the strain of multiple uses may result in the screw heads breaking off.

The slit aperture is sealed with a small O ring held in a Kel-F plunger which is lifted by a modified General Valve armature to generate very reproducible but somewhat long duration (~1–2 ms) gas pulses. The faceplate-electrode assembly is threaded onto valve body, tightened fully, and then loosened "by ear" with the valve driver running. (Valve action is loud in the open chamber.) Next, the volume behind the valve seal is filled with Ar or N_2 to above ambient pressure to check that the valve seals completely, and that during operation, the valve does indeed release gas, lowering the observed pressure in the valved-off feedline. Next the chamber is closed and pumped out to < mTorr with the mechanical pumps. A hearing aid microphone, mounted on a 1/8 inch diameter stainless steel rod and fed through an Ultra Torr fitting, provides a small and effective translatable probe of the gas pulses. The reproducibility and temporal profile of the gas pulses is monitored with this microphone positioned 3–4 cm downstream of the source. Magnitude and duration of the current pulses sent to the solenoid can be adjusted from the driver box to attain full opening of the valve and stable temporal profiles.

The above procedure may need to be repeated to achieve best valve performance but once the optimal tightness of the faceplate is found, there will be a small gap between the faceplate flange and the valve body. Shims are selected from an assortment kept in the lab and installed in this gap. Thereafter, the optimum tightness is reliably reproduced in subsequent re-assemblies of the source. Also, tightened against the shims, the valve faceplate does not loosen due to vibrations during operation.

Once proper valve operation is achieved, high voltage current pulses (*negative* with respect to the grounded valve body) are applied to the slit jaws to form the discharge. To generate the discharge current pulses, a high voltage DC power supply is switched through the same type of circuit used to drive the PZT valve discussed above. The discharge assembly must periodically be disassembled and cleaned when accumulation of discharge products begins to inhibit stable discharge. Fluorine discharge products on the cathode surfaces can be resistant to conventional cleaning solvents and even to concentrated HCl. A solution of HF works well but must be handled with caution – the Special Techniques lab staff can provide instructions and proper equipment.

2.10 Data acquisition and analysis

The FCL is scanned under computer control with the SCANNER program written in Microsoft Visual Basic by Bradley Blackmon. Transient absorption signals are acquired via a transient digitizer or digital oscilloscope, while the DC light level on the signal detector is recorded through a A/D converter and used to convert the signals voltages into absorbance units in the software. Signal and pre-trigger gates are selected in software. TAC fringes are received through another A/D channel and provide the frequency scale for stored laser scans. A fourth data acquisition channel is available for reference cavity absorption signals or alignment signals.[12]

References for Chapter 2

1. D. D. Nelson Jr., A. Schiffman, K. R. Lykke, and D. J. Nesbitt, Chem. Phys. Lett. **153,** 105 (1988).
2. J. L. Hall and S. A. Lee, Appl. Phys. Lett. **29,** 367 (1976).
3. A. Schiffman, Ph. D. Thesis (1993).
4. D. Herriot, H. Kogelnik, and R. Kompfner, Appl. Opt. **3,** 523 (1964).
5. D. Kaur, A. M. de Souza, J. Wanna, S. A. Hammad, L. Mercorelli, and D. S. Perry, Appl. Opt. **29,** 119 (1990).
6. D. Proch and T. Trickl, Rev. Sci. Instrum. **60,** 713 (1989).
7. S. Mackenzie, Private communication (1997).
8. D. M. Neumark, A. M. Wodtke, G. N. Robinson, C. C. Hayden, and Y. T. Lee, J. Chem. Phys. **82,** 3045 (1985).
9. T. Ericson, K. Copeland, and M. Keil, Rev. Sci. Instrum. **65,** 3587 (1994).
10. D. W. Kohn, H. Clauberg, and P. Chen, Rev. Sci. Inst. **63,** 4003 (1992).
11. D. T. Anderson, S. Davis, T. Zwier, and D. J. Nesbitt, Chem. Phys. Lett. **258,** 207 (1996).
12. M. J. Weida, Ph. D. Thesis (1996).